Inorganic Chemistry

Communication

pubs.acs.org/IC

Probing Electrostatic Potential by NMR with the Use of a Paramagnetic Lanthanide(III) Chelate

Eva M. López-Vidal, Martín Regueiro-Figueroa, Marcos D. García, Carlos Platas-Iglesias,* Carlos Peinador,* and José M. Quintela*

Departamento de Química Fundamental, Universidade da Coruña, Campus da Zapateira, Rúa da Fraga 10, 15008 A Coruña, Spain

Supporting Information

ABSTRACT: The paramagnetic complex $[Yb(DOTA)]^-$ forms ion pairs in aqueous solution with cationic species such as *N*-monoalkyl- and *N*,*N*′-dialkyl-4,4′-bipyridinium cations. The magnitude and sign of the induced ^{1}H NMR pseudocontact shift values can be correlated to the electrostatic potential calculated at the MPWLYP/6-311G** level.

The molecular electrostatic potential (MEP)[1] represents a well-established tool for investigating intermolecular interactions, chemical reactivity, and a range of other chemical phenomena.[2] Indeed, it has been shown that electrostatic potentials provide direct insight into intermolecular interactions in crystals,[3] while maps of DNA electrostatic potentials are used as a tool for understanding how proteins recognize binding sites in a genome.[4] Particularly successful is the use of MEPs to rationalize intermolecular interactions involving halogen bonding, that is, interactions where halogen atoms act as electrophilic species.[5] Halogen bonding has been explained by the presence of a region of positive electrostatic potential, the σ hole, on the halogen's surface.[6] The electrostatic potential $V(r)$ that the electrons and nuclei create at any point r in the surrounding space is given in atomic units by

$$V(r) = \sum_A \frac{Z_A}{|R_A - r|} - \int \frac{\rho(r')\,dr'}{|r' - r|} \quad (1)$$

where Z is the charge on nucleus A, located at R_A, and $\rho(r)$ is the electron density of the molecule. The MEP is a quantity observable physically that can be determined experimentally by X-ray diffraction analysis[7] or can be derived directly from the wave function. Experimental electron density distributions are obtained by analysis of the single-crystal X-ray diffraction data measured to ultrahigh resolution, typically to a diffraction resolution limit ~0.5 Å.[8] The main limitations of X-ray ultrahigh resolution diffraction analysis are related to the limited accessibility of the technique, which requires synchrotron radiation, the difficulties often faced to obtain suitable single crystals, and the fact that it can only be applied to the solid state.

Paramagnetic Ln^{III} ions and complexes have been widely used as NMR shift reagents[9] and paramagnetic probes for the structure determination of biomolecules.[10] These paramagnetic probes take advantage of the pseudocontact shifts (PCSs), which result from the dipolar interaction between the (time-averaged) unpaired spin and observed nucleus.[11] In the particular case of axial symmetry, the PCSs are given by

$$\delta_{ij}^{PCS} = D_1 \frac{3\cos^2\theta - 1}{r^3} \quad (2)$$

where r is the Ln−nucleus distance, θ is the angle between the Ln−nucleus vector and the main axis of symmetry of the magnetic susceptibility tensor, and D_1 is proportional to the axial anisotropy of the magnetic susceptibility tensor.

We envisaged that $[Ln(DOTA)]^-$ complexes (DOTA = 1,4,7,10-tetraazacyclododecane-1,4,7,10-tetraacetate) could be suitable paramagnetic compounds to probe positive regions of the electrostatic potential in positively charged species because they were shown to provide significant ion-pair interactions with different cations.[12] Additionally, $[Ln(DOTA)]^-$ complexes present axial symmetry, which simplifies analysis of the PCSs. Among the different Ln^{III} ions, we have selected Yb^{III}, which provides the lowest ratio of the contact to pseudocontact contributions.[11] The electrostatic potential on the molecular surface of $[Yb(DOTA)]^-$ calculated at the MPWLYP/6-311G** level is shown in Figure 1. As noticed previously for related systems,[13] the surface of the complex can be divided into two regions: a hydrophilic region containing the carboxylate groups and characterized by a negative electrostatic potential and a hydrophobic hemisphere on the opposite side of the chelate. Thus, positively charged species are expected to bind $[Yb(DOTA)]^-$ on the hydrophilic side of the molecule. A good agreement was obtained between the ^{1}H paramagnetic shifts observed for

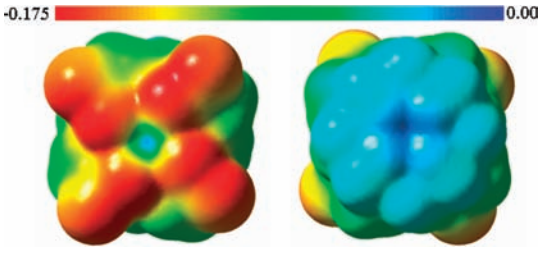

Figure 1. Computed MPWLYP/6-311G** electrostatic potential of $[Yb(DOTA)]^-$ (hartree) on the molecular surface defined by the 0.001 electrons·bohr^{-3} contour of the electronic density. Views are along the molecule C_4-symmetry axis.

Received: February 8, 2012
Published: March 28, 2012

   dx.doi.org/10.1021/ic300288j | *Inorg. Chem.* 2012, 51, 4429−4431

$[Yb(DOTA)]^-$ and those calculated using the MPWLYP/6-311G**-optimized geometry and eq 2 (D_1 = +4406 ± 108 ppm·Å^3; Table S1 in the Supporting Information), which indicates that our density functional theory calculations provide a good model for the structure in solution of this complex. As previously noticed from NMR experiments in solution,[14] the principal magnetic axis of $[Yb(DOTA)]^-$ coincides with the 4-fold symmetry axis of the molecule. The sign of the axial anisotropy is positive, as was expected for ytterbium(III) complexes on the basis of Bleaney's theory.[14,15]

Viologens (4,4′-bipyridinium dication salts), a well-studied class of electron-deficient compounds, have been extensively used as components in many supramolecular structures because of their electrochemical behavior and electronic properties.[16] Thus, we selected a series of *N*-monoalkyl- and *N*,*N*′-dialkyl-4,4′-bipyridinium salts with potentially different charge topologies to investigate their electrostatic potential with the use of $[Yb(DOTA)]^-$ and computational methods (Chart 1). Some of

Chart 1. *N*-Monoalkyl- and *N*,*N*′-Dialkyl-4,4′-bipyridinium Species Investigated in This Work

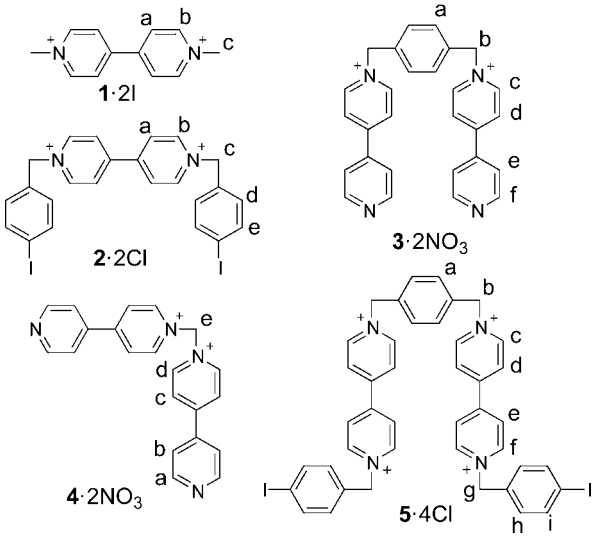

the substrates selected were commercially available (**1**) or were prepared following previously reported procedures (**2**,[17] **3**,[18] and **4**[19]). In addition, we have synthesized the new compound **5**, which was isolated as the chloride salt.

The addition of $[Yb(DOTA)]^-$ to aqueous solutions of compounds **1**−**5** results in significant changes in their ^{1}H NMR shifts (Figure 2). Only one set of resonances was observed for the corresponding viologen, indicating rapid exchange between the bound and unbound forms of the substrate on the NMR time scale. Under these conditions, the observed chemical shift δ is the average of the chemical shifts of the free and bound forms of the viologen weighted by their fractional populations. The titration data presented in Figure 2 show that some proton signals undergo considerable shifts toward lower fields upon the addition of $[Yb(DOTA)]^-$, while for other signals, the chemical shifts are little affected or even experience shifts to higher fields. This result points to a rather specific interaction between the paramagnetic probe and the substrates. Because of the $1/r^3$ dependence of the PCS (eq 2), larger paramagnetic shifts are expected for those protons placed closer to the Yb^{III} ion. In addition, the 3 $\cos^2\theta - 1$ term in the numerator of eq 2 defines a magic-angle cone surface

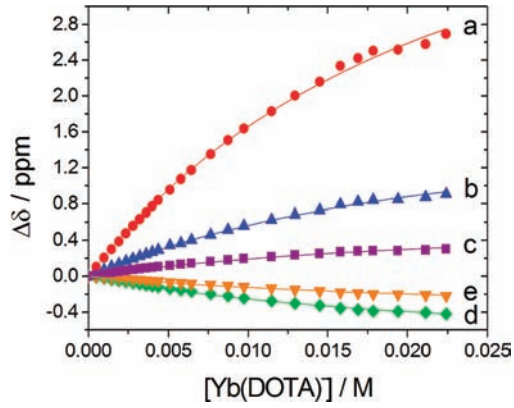

Figure 2. Titration curves showing the ^{1}H NMR chemical shifts of **2** (2.9 mM) induced by $[Yb(DOTA)]^-$. Solid curves represent fits of experimental data according to a 1:1 binding model with K_{11} = 48 ± 1.

for θ = 54.7°. Any proton nucleus inside this cone surface is shifted to high frequency (lower fields) and therefore should provide positive Yb^{III}-induced PCSs. On the contrary, those proton nuclei placed outside the cone would be shifted to higher fields. Considering that the region of $[Yb(DOTA)]^-$ where the carboxylate functions are placed is characterized by a negative electrostatic potential and the position of the C_4 axis (Figure 1), one would expect that the signals of those proton nuclei of compounds **1**−**5** placed in regions with positive electrostatic potential would undergo shifts to lower fields. Thus, large positive Yb^{III}-induced shifts ($\Delta\delta$) identify those regions on the surface of the molecule characterized by positive electrostatic potentials.

The ^{1}H NMR titration data were satisfactory fitted to a 1:1 binding model, which allowed us to determine the association constants characterizing the ion pairs formed between $[Yb(DOTA)]^-$ and the substrates, as well as the corresponding bound shifts (Δ). The association constants obtained, which range from 26 ± 1 M^{-1} for **1** to 55 ± M^{-1} for **4**, are similar to those determined for ion pairs formed between $[Tm(DOTA)]^-$ and a positively charged lanthanum(III) chelate.[12]

Figure 3 shows the electrostatic potential on the molecular surfaces of compounds **2**−**4** at the MPWLYP/6-311G** functional level, defined by the 0.001 electrons·bohr^{-3} contour of the electron density following the suggestion of Bader et al.[20] The electrostatic potential on these surfaces is completely positive, as was expected because of the positive charges of the molecules. The most positive electrostatic potential on the molecular surfaces of *N*,*N*′-dialkyl-4,4′-bipyridinium derivatives **1**, **2**, and **5** is located at the H atoms of the bipyridinium unit (Figures 3 and S11 in the Supporting Information). However, the most positive electrostatic potential on the surfaces of *N*-monoalkyl derivatives **3** and **4** is located close to the methylenic H atoms and the H atoms of the neighboring pyridinium units.

Those regions on the molecular surface of the cations with the highest electrostatic potential (shown in blue in Figure 3) clearly correlate with the largest Δ values obtained from analysis of the ^{1}H NMR titration data. On the contrary, protons in those regions with lower positive electrostatic potentials present small positive (or even negative) bound shifts. This is attributed to the relatively long distance from these protons to the paramagnetic probe and the fact that they are placed close to (or outside) the cone surface given by the magic angle. Thus, we conclude that the paramagnetic $[Yb(DOTA)]^-$ probe is able to identify those regions with the highest positive electrostatic potential in these cations.

dx.doi.org/10.1021/ic300288j | *Inorg. Chem.* 2012, 51, 4429−4431

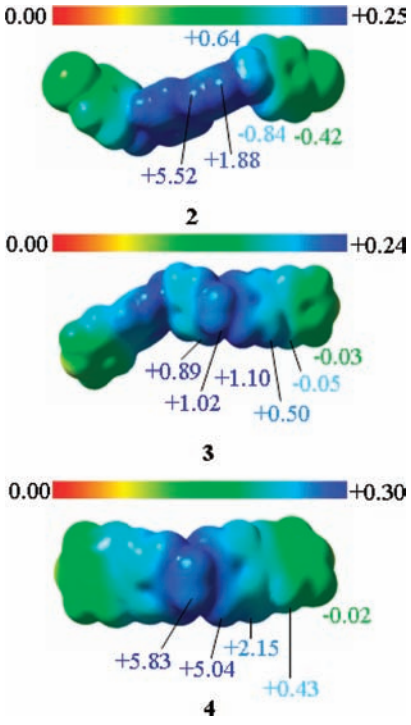

Figure 3. Computed MPWLYP/6-311G** electrostatic potential of cations **2**–**4** (hartree) on the molecular surface defined by the 0.001 electrons·bohr^{-3} contour of the electronic density and bound shifts (Δ, ppm) determined from analysis of the NMR titration data.

The addition of an excess of **1** to a solution of [Yb(DOTA)]$^-$ in D_2O provokes very few changes in the ^{1}H NMR shifts of the paramagnetic probe (<1 ppm), which indicates that the magnetic anisotropy of the ytterbium(III) complex remains nearly unaffected by interaction with the cation. Considering a typical bound shift of 6 ppm for the most shifted resonance of viologens **2** and **4** (Figure 3), associated with θ values of 20–50° and D_1 = +4406 ppm·Å^3, one can estimate a Yb···H distances in the range of 10.7–5.6 Å. Ln···C distances of 4.1–6.2 Å have been determined for adducts formed between [Tm(DOTA)]$^-$ and positively charged lanthanum(III) complexes.[12] This suggests that in the case of compounds **2** and **4** the average θ value for the protons giving the most shifted resonances is close to 50°.

In conclusion, we have developed an experimental method that allows us to explore the regions with positive electrostatic potential on the surface of positively charged species. The method is very simple because it actually requires one to compare the ^{1}H NMR spectrum of the cation in water in the absence and in the presence of an excess of [Yb(DOTA)]$^-$. Furthermore, the magnitudes of the bound shifts could be controlled by using other Ln^{III} ions, such as Tm^{III}, that provide larger induced paramagnetic shifts. The association constants of the ion pairs formed in solution could also be increased by using a paramagnetic probe with a higher negative charge, for instance by replacing the acetate arms of DOTA by methylenephosphonate groups.[21]

■ ASSOCIATED CONTENT

Supporting Information

Synthesis and spectroscopic data of **5**·4Cl, ^{1}H NMR titration curves of **1** and **3**–**5**, and optimized Cartesian coordinates of compounds **1**–**5** and [Yb(DOTA)]$^-$. This material is available free of charge via the Internet at http://pubs.acs.org.

■ AUTHOR INFORMATION

Corresponding Author

*E-mail: carlos.peinador@udc.es (C.P.), carlos.platas.iglesias@udc.es (C.P.-I.), jose.maria.quintela@udc.es (J.M.Q.).

Notes

The authors declare no competing financial interest.

■ ACKNOWLEDGMENTS

This research was supported by Ministerio de Educación y Ciencia and FEDER (Grant CTQ2010-16484/BQU). E.M.L.-V. thanks the Ministerio de Ciencia e Innovación (FPI program). The authors thank CESGA for providing the computer facilities.

■ REFERENCES

(1) Murray, J. S.; Politzer, P. *WIREs Comput. Mol. Sci.* **2011**, *1*, 153–163.
(2) Merino, G.; Vela, A.; Heine, T. *Chem. Rev.* **2005**, *105*, 3812–3841.
(3) (a) Spackman, M. A.; McKinnon, J. J.; Jayatilaka, D. *CrystEngComm* **2008**, *10*, 377–388. (b) Rohde, D.; Yan, C.-J.; Wan, L.-J. *Langmuir* **2006**, *22*, 4750–4757.
(4) Bishop, E. P.; Rohs, R.; Parker, S. C. J.; West, S. M.; Liu, P.; Mann, R. S.; Honig, B.; Tullius, T. D. *ACS Chem. Biol.* **2011**, *6*, 1314–1320.
(5) Metrangolo, P.; Meyer, F.; Pilati, T.; Resnati, G.; Terraneo, G. *Angew. Chem., Int. Ed.* **2008**, *47*, 6114–6127.
(6) (a) Clark, T.; Hennemann, M.; Murray, J. S.; Politzer, P. *J. Mol. Model.* **2007**, *13*, 291–296. (b) Politzer, P.; Lane, P.; Concha, M. C.; Ma, Y.; Murray, J. S. *J. Mol. Model.* **2007**, *13*, 305–311.
(7) (a) Fournier, B.; Bendeif, E.-E.; Guillot, B.; Podjarny, A.; Lecomte, C.; Jelsch, C. *J. Am. Chem. Soc.* **2009**, *131*, 10929–10941. (b) Lecomte, C.; Guillot, B.; Jelsch, C.; Podjarny, A. *Int. J. Quantum Chem.* **2005**, *101*, 624–634.
(8) Jelsch, C.; Teeter, M. M.; Lamzin, V.; Pichon-Pesme, V.; Blessing, R. H.; Lecomte, C. *Proc. Natl. Acad. Sci. U.S.A.* **2000**, *97*, 3171–3176.
(9) Aspinall, H. C. *Chem. Rev.* **2002**, *102*, 1807–1850.
(10) (a) Rao, N. *J. Am. Chem. Soc.* **1988**, *110*, 8275–8287. (b) Allegrozzi, M.; Bertini, I.; Janik, M. B. L.; Lee, Y.-M.; Liu, G.; Luchinat, C. *J. Am. Chem. Soc.* **2000**, *122*, 4154–4161. (c) Barry, C. D.; North, A. C. T.; Glasel, J. A.; Williams, R. J. P.; Xabier, A. V. *Nature* **1971**, *232*, 236–245.
(11) Peters, J. A.; Huskens, J.; Raber, D. J. *Prog. NMR Spectrosc.* **1996**, *28*, 283–350.
(12) Corsi, D. M.; van Bekkum, H.; Peters, J. A. *Inorg. Chem.* **2000**, *39*, 4802–4808.
(13) Borel, A.; Helm, L.; Merbach, A. E. *Chem.—Eur. J.* **2001**, *7*, 600–610.
(14) Aime, S.; Botta, M.; Ermondi, G. *Inorg. Chem.* **1992**, *31*, 4291–4299.
(15) Bleaney, B. *J. Magn. Reson.* **1972**, *8*, 91–100.
(16) (a) Balzani, V.; Credi, A.; Raymo, F. M.; Stoddart, J. F. *Angew. Chem., Int. Ed.* **2000**, *39*, 3348–3391. (b) Monk, P. The Viologens: Physicochemical Properties. *Synthesis and Applications of the Salts of 4,4′-Bipyridine*; Wiley: New York, 1998.
(17) García, M. D.; Blanco, V.; Platas-Iglesias, C.; Peinador, C.; Quintela, J. M. *Cryst. Growth Des.* **2009**, *9*, 5009–5013.
(18) Anelli, P. L.; Ashton, P. R.; Ballardini, R.; Balzani, V.; Delgado, M.; Gandolfi, M. T.; Goodnow, T. T.; Kaifer, A. E.; Philp, D. *J. Am. Chem. Soc.* **1992**, *114*, 193–218.
(19) Blanco, V.; Chas, M.; Abella, D.; Pia, E.; Platas-Iglesias, C.; Peinador, C.; Quintela, J. M. *Org. Lett.* **2008**, *10*, 409.
(20) Bader, R. F. W.; Carroll, M. T.; Cheeseman, J. R.; Chang, C. *J. Am. Chem. Soc.* **1987**, *109*, 7968–7979.
(21) Ren, J.; Springer, C. S. Jr.; Sherry, A. D. *Inorg. Chem.* **1997**, *36*, 3493–3498.